Journal of Polymers and the Environment (2025) 33:1517–1527
https://doi.org/10.1007/s10924-024-03360-z

ORIGINAL PAPER

Improving rPET/PBT Bead Foam Structure via Chain Extender Modification and Blend Variance

Andreas Himmelsbach[1] · Yavuz Akdevelioglu[2] · Mohammadreza Nofar[2] · Holger Ruckdäschel[1]

Accepted: 7 July 2024 / Published online: 11 January 2025

Abstract

In this study, the influence of the chain extender (CE) and the blend ratio on the bead foam extrusion of rPET/PBT is investigated. The shape and density of the bead foams were analyzed during extrusion using a camera scanner while the morphology of the foam was investigated using scanning electron microscopy (SEM). Melt strength and thermal behavior were also investigated with Rheotens and differential scanning calorimetry (DSC), respectively. Both chain extender and blend ratio had pronounced effect on the foaming behavior. Significant improvements were observed up to 0.8 wt.-% CE in rPET50PBT50, which achieved an average cell size of 107 ± 17 µm and a density of 182 kg/m³, representing a weight reduction of 86.4% compared to the bulk material. In addition, rPET40PBT60 with 0.8 wt.-% CE gave an average cell size of 108 ± 23 µm and a foam density of 170 kg/m³, with a comparable cell size distribution. After CE modification, the melt strength of rPET-dominant blends obtained higher values but a strong decrease in elongation was observed. In contrast, the CE-modified rPET40PBT60 and rPET30PBT70 blends exhibited much higher elongation with a moderate increase in melt strength which resulted in better bead and foam morphologies. DSC analysis revealed lowest crystallization temperature in rPET50PBT50 with deviations shifting towards higher temperatures. All blends except rPET70PBT30 shows double melting peak formation, with higher rPET formulations also exhibiting cold crystallization. These findings provide crucial insight for development of rPET/PBT foams by controlling the blend and CE composition, which is critical for achieving temperature-resistant bead foams with improved structural integrity.

Graphical Abstract

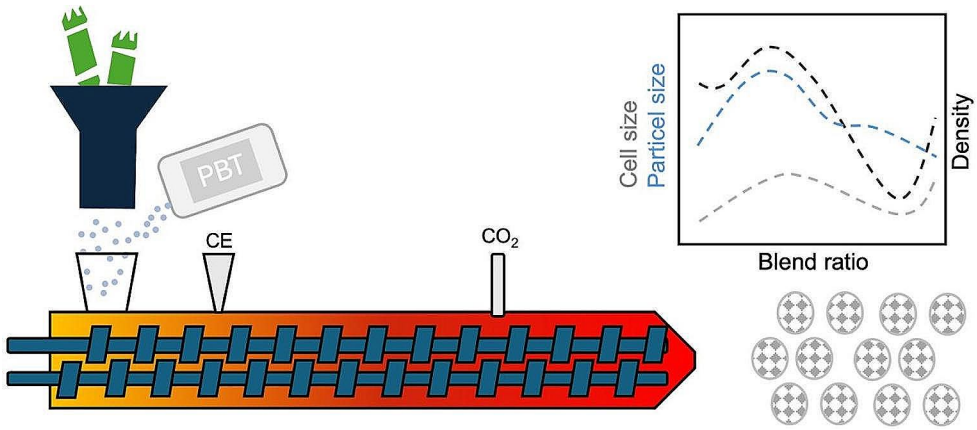

Keywords Recycled polyethylene terephthalate · Polybutylene terephthalate · Joncryl · Bead foaming · Reactive extrusion

Extended author information available on the last page of the article

Introduction

Polybutylene terephthalate (PBT) bead foams represent an innovative and lightweight material, distinguishing themselves from conventional expandable polystyrene (EPS) [1] and expanded polypropylene (EPP) [2] due to its higher heat stability [3]. Focusing on the exceptional mechanical, thermal, and chemical properties of PBT, these foams could find versatile applications in packaging, construction, and specialized industries [3–6].

Previous studies have successfully demonstrated the manufacture of PBT beads through reactive foam extrusion. Processing parameters (temperature, screw speed, water pressure, etc.) and formulation components (molecular weight, viscosity, chain extender, and blowing agent content) play a pivotal role [6–10].

The importance of viscosity for successful foaming of linear polyester, especially PBT, has been emphasized in the literature [7–9, 11–17], as it significantly influences both cell stabilization and growth. Inadequate viscosity leads to cell coalescence and fracture, while increased viscosity results in more spherical beads and promotes homogenous, finer cells due to a reduced growth rate [8, 9].

In literature two strategies were employed to enhance viscosity of PBT. As a first strategy, an investigation of linear PBT with varying molecular weights revealed a correlation following the Mark-Houwink equation [18]. Optimal foam density and cell density were achieved for a viscosity of 557 Pa*s. With increased viscosity corresponding to higher densities, while reduced molecular weight yielded larger, less uniform morphologies [9]. As a second common strategy, the addition of a CE aims to create a branched/cross-linked structure, enhancing melt strength [8, 19–21]. Optimal conditions for lowest density (179 kg/m$^{3)}$ and homogeneous cell structure (155 µm) were observed for PBT containing 1.0 wt.-% CE [8]. However, higher concentrations of the chain extender increased viscosity to levels where shear forces caused degradation, in turn leading to a reduction in final viscosity [8, 22].

Standau et al. [6]. and Köppl et al. [7]. demonstrated the potential of optimizing density and morphology by adjusting in process parameters. Increasing throughput leads to higher die pressure and melt temperature due to increased shear, resulting in a more significant pressure drop that influenced nucleation and expansion. Moreover, higher throughput with increased water temperature resulted in a bead foam with a density of 85 kg/m^3 and fine cell morphology [6].

Blending different polymers is a frequently used method to improve certain properties and thus increase foamability [17, 23–27]. In a study by Mielke et al. [26]., the addition of 2 to 8% by weight of poly(butylene furanoate) (PBF) has a remarkable effect on the morphology of PBT bead foam, which has a finer and more uniform cell structure. Their work highlights the feasibility of welding, an important step in the processing of bead foam, which is attributed to a double melting peak within the material [26]. In similar manner, Brütting et al. [25]. observed reduced cell size by blending poly(lactic acid) (PLA) with poly(3-hydroxybutyrate-co-3-hydroxyvalerate) (PHBV). This echoes findings in prior research on PET/PC [17] and LPP/HPP [27] blends, indicating enhanced density and improved morphology through blending.

The steam chest molding process, especially for polyesters such as PBT, is known for a relatively narrow processing window [7, 28, 29]. Moreover, conventional steam molding methods face challenges due to the high welding temperature of PBT, making them energy intensive. Dippold et al. [30]. demonstrated the feasibility of welding PBT using an radio frequency (RF) process. Through blending PBT with miscible or compatible polymers, the welding window could be expanded. The addition of PET, for instance, introduces a double melting peak, offering advantages for the welding process [23, 24, 31, 32]. The broader melting range also positively impacts the processability via the RF process [30].

In a previous investigation, the crystallization behavior of rPET/PBT blends was explored [33]. The study revealed that blending both polymers generated a double melting peak across a wide blending range. Consequently, the processing window in the RF process could be extended from 4 K to 30 K. Moreover, blending resulted in a reduction of the crystallization temperature, as the separation of both polymers precedes crystallization. This significant reduction was particularly notable for the rPET50PBT50 blend. Additionally, the mixing process led to a decrease in crystallization rate of PBT. The combination of a lower crystallization temperature and a slower crystallization rate contributes to a higher expansion rate during bead foaming.

In another preceding study, the impact of rPET on the rheological properties of PBT was examined [32]. It is known that the viscosity of unmodified PBT decreases as the rPET content increases. This phenomenon is attributed to the distinct molecular weights between the virgin and recycled components [34]. The melt strength of PBT, a critical property in terms of foaming, diminishes upon blending, while the drawability of the material increases [8, 19, 35, 36]. Additionally, it was observed that, rPET typically undergoes polycondensation reactions during processing, resulting in a higher Melt Flow Rate (MFR) [24]. However, this effect could be mitigated by the presence of the PBT phase in the blend.

In a nutshell, the foamability of rPET/PBT blends and the impact of rPET on the morphology of PBT extrusion bead

foams have not been investigated yet. This study seeks to analyze the influence of rPET of various parameters, including cell size, particle size, foam density, and melt elongation behavior of rPET/PBT bead foams.

Experimental Section

Materials

PBT Pocan B1300, sourced from Lanxess AG (Cologne, Germany), possesses a glass transition temperature (T_g) of 48 °C and a melting peak spanning from 216 to 227 °C, with a weight average molecular weight (M_w) of 66,000 g/mol. The PET recycled from soft drink bottles, provided by Arcelik A.S. (Istanbul, Turkey), has a semi-crystalline nature, with a M_w of 44,000 g/mol and a T_g of 77 °C. Both polymers were dried for at least 12 h at 120 °C before the foam extrusion. The CE employed was the multifunctional epoxy-based Joncryl ADR 4468 sourced from BASF (Ludwigshafen, Germany). This modifier has a M_w of 7,250 g/mol and an epoxy equivalent weight of 310 g/mol, exhibiting a T_g at 59 °C [21].

Processing

Bead foams were manufactured using a Dr. Collin tandem foam extrusion line (Ebersberg, Germany), in conjunction with an underwater granulator (UWG) LPU provided by Gala Kunststoff- und Kautschukmaschinen GmbH (Xanten, Germany).

The tandem line included a twin-screw extruder (diameter D = 25 mm, L/D ratio = 42D). Here, the dry blends, incorporating various concentrations of chain extender and the blowing agent CO_2 (40 bar), underwent blending at 265 °C with a screw speed of 150 rpm. The resulting one-phase gas-melt mixture was then directed to the subsequent single-screw extruder (Diameter = 45 mm, L/D ratio = 30D), where the gas-loaded melt underwent controlled cooling to 255 °C. To ensure process stability, the screw speed was adjusted of 11 rpm, responding to changes in melt pressure.

In the connected underwater granulator, the gas-loaded melt was extruded through a die plate at a temperature of 280 °C, instigating the foaming process as the pressure decreased. Simultaneously, a rotating knife (1600 rpm) cut the expanding polymer strand into foamed beads. These beads were transported by a continuous water stream (80 °C), subjected to drying, and subsequently discharged from the machine. The production throughput was maintained at 6.0 kg/h.

Bead Morphology and Density

The foam morphology of individual beads was investigated using a JEOL JSM-6510 scanning electron microscope (SEM) (Akishima, Japan), operating at 1.5 kV and platinum covered samples of 0.8 nm thickness. The obtained images were then analyzed using ImageJ software. To assess cell density, cell sizes, and cell size distributions, two beads per rPET/PBT formulation were examined.

The density and particle shape of the beads were measured using the CAMSIZER 3D from Microtrac (Haan, Germany). The sample was weighed and recorded in the software. Several photographs were taken of each bead as it fell through the measuring section. From these, the software calculates the volume of a sphere of comparable diameter. The density of the samples is calculated from the total mass and the averaged volume. The recorded data was then analysed using the PartAn3DPro software.

Melt Strength

Rheotens measurements were carried out in conjunction with a capillary rheometer to evaluate the melt strength. The beads were placed in the cylinder, melted at 255 °C and then extruded through a capillary (length = 30 mm, diameter = 2 mm) using the Rheograph 75 from Göttfert Werkstoff-Prüfmaschinen GmbH (Buchen, Germany) for the rPET50PBT50. To compare the melt strength of the different blend systems, a capillary (length = 30 mm, diameter = 1 mm) must be used due to the low viscosity of the rPET-dominant blends. All blend formulations were tested for comparison purposes at a temperature of 255 °C, which corresponds to the die temperature during extrusion. The strand was extruded at a controlled speed of 0.174 mm/s and stretched between 25 and 500 mm/s with an acceleration of 12 mm/s² by the two counter-rotating wheels of the Rheotens 71.97 device. The pairs of wheels, which were connected to a force transducer, continuously measured the tensile force exerted on the stretched extrudate.

Differential Scanning Calorimetry

The crystallization behavior of the rPET/PBT blends was analyzed using a Mettler Toledo differential scanning calorimeter (DSC1) (Columbus, USA). Samples underwent two heating and one cooling cycle between 25 and 280 °C at a rate of 10 K/min. Calculations for the degree of crystallinity were based on the heating thermograms, factoring in the theoretical heat of fusion for both rPET and PBT (ΔH°_{f} = 140 J/g) [37].

Results and Discussion

Effect of Chain Extender Content on rPET50PBT50 bead Foams

The effect of CE on the foamability of rPET50PBT50 blends was initially investigated to determine the most effective concentration for achieving low density and a refined cell structure. It is known, that the CE plays a crucial role in increasing the viscosity and melt strength of linear polyester and thus foamability [8, 15, 19, 38, 39]. Prior studies pinpointed a 0.75 wt.-% CE concentration as the most effective in modifying viscosity [32]. Lower concentrations, such as 0.25 wt.-%, only compensated for chain scissoring, while a 1.0 wt.-% concentration already increased the viscosity to a level that could lead to shear degradation. Moreover, sharp increase in melt strength due to strain hardening at 1.0 wt.-% reduces foamability while below 0.5 wt.-% has unremarkable strain hardening behavior [8, 32, 40, 41]. Therefore, in this study, the CE concentration was varied from 0.5 to 0.8 wt.-%, with the concentrations of unmodified (0 wt.-%) and 1.0 wt.-% CE serving as reference points.

The results for the foaming of rPET50PBT50 under variation of the CE content are summarized in Table 1. Notably, the melt pressure exhibits an increase from 49 bar (0 wt.-% CE) to 157 bar for a modification of 0.8 wt.-% CE. This increase in die pressure can be attributed to the CE reaction. As the CE content increases, the proportion of long-chain branched structures increases, which leads to increased melt strength and strain hardening [8, 19, 40]. At the same time, a higher die pressure also leads to a higher pressure drop and thus to increased foam nucleation [6, 7]. Both effects, higher melt strength and greater pressure drop, can lead to a more homogeneous and finer cell structure. However, a further rise in CE content surprisingly results in a significant reduction in pressure to 92 bar (1.0 wt.-% CE). This trend is related to the possibility of shear-induced degradation at a certain level of long-chain branching [8, 42]. Additionally, significant strain hardening leading to reduced elongation can result in cell rupture, while extensive branching and high gel content may diminish gas absorbability [32].

According to literature [7, 39, 43], the pressure drop at the nozzle plays a crucial role in nucleation and cell growth, influencing the average cell size. In general, wherein higher melt pressure tends to yield smaller cells (see Table 1). The unmodified blend shows an inhomogeneous morphology (see supporting information S1), which shows how difficult it is to achieve a uniform cell size distribution. The addition of CE significantly reduces both average cell size and uniformity. In an earlier study with the related polyester PBT, it was shown that the cell structure can be changed by adjusting the viscosity [22]. Similar results were obtained by Kunigkh et al. [9]. Notably, the blend treated with 0.8 wt.-% CE shows the smallest cell size, which is 107 ± 17 µm.

Figure 1 illustrates the cell size distributions of various rPET50PBT50 foams through box plots, encapsulating values within 1.5 standard deviations from the median while excluding outliers. The increase in CE correlates consistently with a reduction in average cell size, particularly clearly in the range of 0.6 to 0.8 wt.-% CE. The narrower box plots signify the more homogenous cell size distribution. This trend aligns with the observed rising melt pressure, potentially contributing to higher foam densities, a pattern observed in prior studies involving PBT [8, 9], PC [44], and PLA [11, 25]. Interestingly, the median value shifts towards the upper end of the box with increasing CE content, indicating that more than half of the cells are smaller than the calculated mean value. The closeness between the median and mean indicates a remarkably homogeneous morphology. It is noteworthy that outliers within the 0.8 wt.-% CE modification fall within the standard deviation range observed in 0.6 and 0.7 wt.-% CE modified foams. However, at 1.0 wt.-% CE, a broader cell size distribution suggests a more heterogeneous morphology (see supporting information S1 and S2), highlighted by notable discrepancies between mean and median values. Nevertheless, the overall morphology shows progress compared to the 0.5 wt.-% CE modification. Even if the melt pressure is significantly lower (see Table 1), and thus, the melt viscosity should also be lower in the case of 1.0 wt.-% CE modifications [8].

The optimal formulation for achieving the desired cell size is found in rPET50PBT50 modified with 0.8 wt.-% CE.

Table 1 Output parameter of rPET50PBT50 bead foaming with varied CE content

CE content wt.-%	T_{melt} °C	p_{melt} bar	Density[1] kg/m³	Particle size[1] mm	Cell size[2] µm	$F_{melt}^{3/4}$ N
0.0	244	49	254	4.72 ± 0.33	n.d.	n.d.
0.5	250	122	192	5.18 ± 0.19	165 ± 25	0.0015
0.6	258	133	174	5.34 ± 0.18	124 ± 22	0.0070
0.7	258	139	195	5.14 ± 0.18	115 ± 17	0.0080
0.8	257	157	182	5.28 ± 0.19	107 ± 17	0.0131
1.0	253	92	153	5.98 ± 0.31	157 ± 42	n.a.

[1]Measured with CamSizer 3D, [2]Measured with SEM, [3]round hole die with 30/2 mm used, [4]see supporting information S7

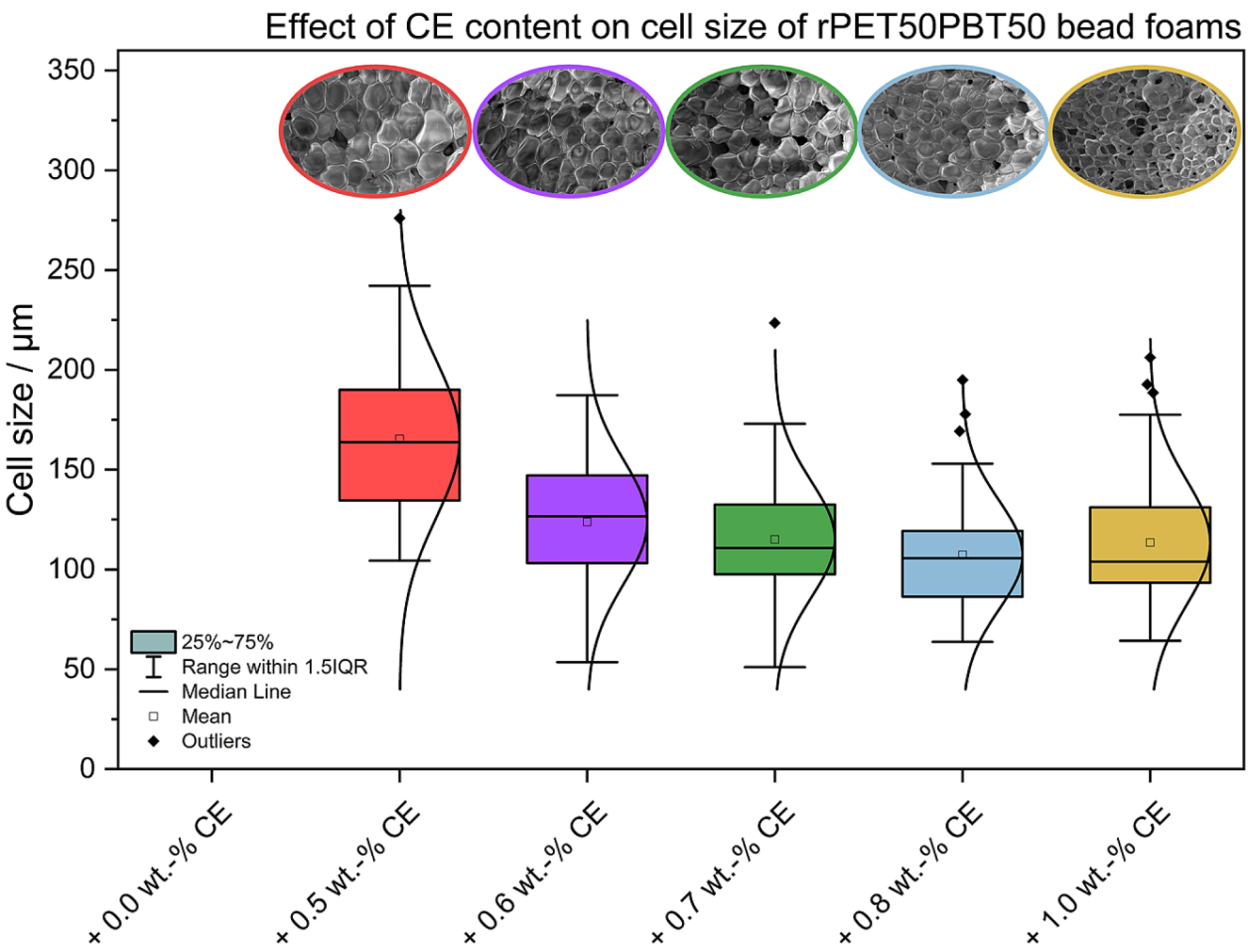

Fig. 1 Effect of CE content on cell size of rPET50PBT50 bead foams

If the two reference points (0 wt.-% and 1.0 wt.-% CE) are disregarded due to their corresponding heterogeneous morphology, the lowest density is achieved with a 0.6 wt.-% modification. It is known that a reduction in cell size generally leads to an increase in density. Both 0.6 and 0.8 wt.-% CE result in a weight reduction of 87.0% and 86.4%, respectively. As suggested in previous publications, the optimal balance between density and cell size is expected to be in the range of 0.7 to 0.8 wt.-% CE modification [32].

Effect of rPET-PBT Blend Ratio on the foam Morphology

The influence of the blend ratio on the foamability and morphology of rPET-PBT bead foams is investigated. Therefore, 0.8 wt.-% CE was chosen. In a next step, the best processing conditions found for rPET50PBT50 blends are used and consistently maintained throughout the experiments. Since the thermal and rheological properties of the two polymers are quite different, only blends between rPET70PBT30 and rPET30PBT70 can be investigated. Furthermore, it is known that blending rPET with PBT causes significant changes in crystallization and rheological behavior, suggesting possible effects on foam morphology [24, 45–47].

Table 2 Results of rPET-PBT bead foaming with varied blend ratio

	T_{melt} °C	p_{melt} bar	Density[1] kg/m³	Particle size[1] mm	Cell size[2] µm
rPET30PBT70	256	142	194	5.47 ± 0.19	101 ± 27
rPET40PBT60	257	152	170	5.66 ± 0.20	108 ± 23
rPET50PBT50	257	157	182	5.28 ± 0.19	107 ± 17
rPET60PBT40	257	160	208	5.19 ± 0.16	102 ± 21
rPET70PBT30	256	194	234	5.03 ± 0.16	130 ± 31

[1]Measured with CamSizer 3D, [2]Measured with SEM

The data from the extrusion process, including melt temperature and pressure, as well as the results related to the morphology of individual beads, are summarized in Table 2. While the melt temperature remains stable across different blend ratios, an increase in melt pressure can be observed with higher rPET content. In particular, rPET70PBT30 has exhibits the highest melt pressure at 194 bar, while

rPET30PBT70 has the lowest pressure at 142 bar. This variation can be attributed to the different melting ranges of rPET and PBT. PBT melts at a peak temperature of 227 °C, while this phase transition occurs at a higher temperature of 257 °C for rPET [33]. The discrepancy results from the structural differences and the higher oxygen-to-carbon ratio per repeat unit in rPET, which may contribute to improved crystal perfection. It is known that blending lowers the melting point [46, 48, 49], as the presence of the blending partner restricts the movement of the chain segments. Consequently, the melting temperature of rPET is lowered to 245 °C (rPET70PBT30) and 231 °C (rPET30PBT70) (see Table 3). In the context of the blend system, the observed increase in melt pressure with increasing rPET content cannot be attributed to the increased viscosity in formulations with higher rPET content [32]. However, given the simultaneous tendency towards increasing particle size and decreasing melt pressure, it can be assumed that there may be differences in rheological properties at these temperatures.

The lowest density for all blends was observed for rPET40PBT60 at 170 kg/m^3. However, in contrast to the experiments with different CE concentrations, no recognizable correlation between density and melt pressure could be found. With increasing rPET content, the density of the foam increases continuously, which is primarily due to a lower absorption of the blowing agent absorption. Conversely, the highest density of 234 kg/m^3 was determined in rPET70PBT30. Interestingly, an increase in density with increasing PBT content can be observed in rPET40PBT60, leading to a bead density of 194 kg/m^3. Both phenomena can be attributed to the selected process conditions. Please note that the conditions were set for rPET50PBT50 were fixed and kept constant for the comparability of the results. In the case of the rPET-dominant blend, the process temperature is already too low, and the melt is inhibited in its expansion. In the case of the PBT-dominant blend, the temperature is too high and the cells can collapse.

The effect of the blend ratios on the foam morphology, in particular the cell size, are shown in Fig. 2. It can be seen, that the average cell size remains relatively constant between the blend ratios of rPET70PBT30 to rPET40PBT60. However, with a further increase in PBT content, there is a significant increase in the average cell size to 130 ± 31 µm. This increase is attributed to improved drawability (refer to Fig. 3), which enables greater expansion in formulations where PBT plays a dominant role.

While the average cell size changes only slightly in the blends, there is a clear effect in the distribution of cell size. The formulations with the greatest differences in blend ratio exhibit the most heterogeneous morphologies. In the PBT-dominant blend, the cell sizes deviate significantly from the average, with above average cell size. In contrast, the pattern is reversed in the rPET-dominant blend. This deviation correlates with the measured melt strengths. rPET70PBT30 has a relatively high melt strength (0.032 N) but a limited expansion capacity, which favors cell nucleation over expansion [27]. In contrast, rPET30PBT70 has a relatively high elongation, indicating more favorable expansion conditions (see Fig. 3). rPET50PBT50 has a supposedly more homogeneous morphology. However, it is important to note that outliers, i.e. cells that deviate 1.5 times from the mean, are not considered in this analysis. In contrast, the rPET40PBT60 formulation has the most uniform morphology with a cell size of 108 ± 23 µm. This uniformity can be attributed, in part, to the rheological properties (see Fig. 3) and the relatively rapid onset of crystallization (see Fig. 4) [15, 38, 50, 51].

Figure 3 illustrates the melt strength of the foamed and remelted blends with different blend compositions. It is obvious that, both the strength and the maximum melt elongation decrease with increasing rPET content (see Table 3). This phenomenon can be attributed to the lower molecular weight of rPET compared to PBT, which leads to a lower entanglement density in rPET [23, 24, 32]. A similar trend was reported by Akdevelioglu et al. [32]. The deviation in the trend observed for rPET70PBT30 can be attributed to the low temperature at which the tests were performed. The measurement range is close to the melting range of rPET, indicating the possible presence of residual crystallinity. For reasons of comparability, the tests were conducted at this temperature (refer also to process temperature). An overview of the thermal and rheological properties of the foams tested can be found in Table 3.

Blending rPET with PBT aims to improve foamability and weldability by creating a double melting point, thereby extending the processing window. Figure 4a shows that,

Table 3 Thermal behavior and rheological properties of rPET-PBT bead foam with varied blend ratio

PBT content wt.-%	T_c °C	T_{mPBT} °C	T_{mrPET} °C	T_{cc} °C	X_{PBT} °C	X_{rPET} °C	F_{melt}[1] *N*	Drawability[1] 1
30	165	–	245	98	–	6.6	0.032	12.0
40	142	206	236	81	9.7	7.3	0.009	17.7
50	152	207	232	82	15.6	5.1	0.014	18.7
60	172	210	232	–	22.5	6.9	0.016	34.7
70	175	215	231	–	27.8	3.9	0.022	33.7

[1]Round hole die with 30/1 mm used

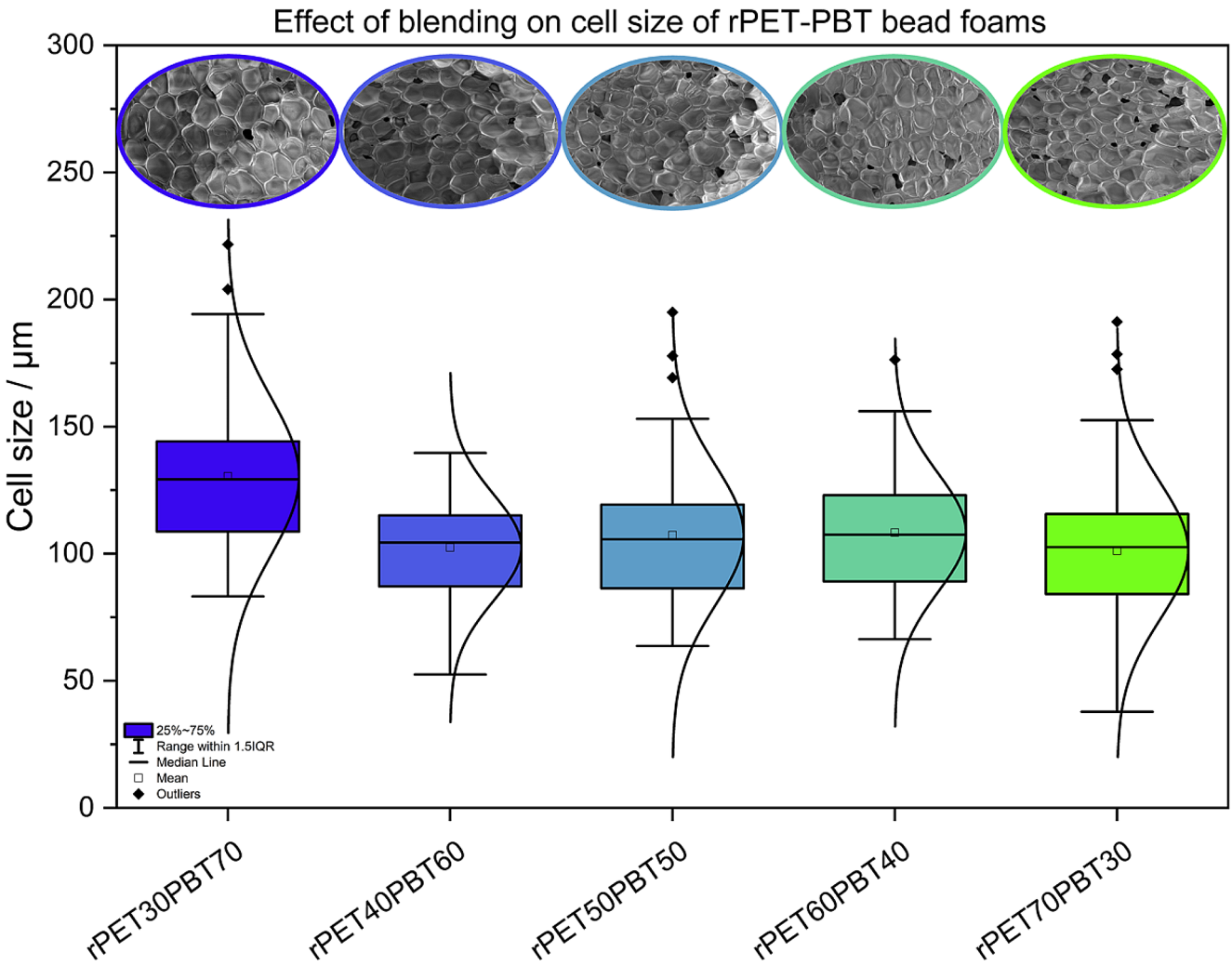

Fig. 2 Effect of blend ratio on foam morphology of rPET-PBT foams modified with 0.8 wt.-% CE

with the exception of rPET70PBT30, all formulations exhibit a double melting peak during rapid cooling after the extrusion process. Two observations are can be made from these data. Firstly, the cold crystallization of rPET decreases with the addition of PBT. This can be attributed to the lower T_g and the improved chain mobility resulting from the lower viscosity of the blend [33, 48, 52]. Secondly, both melting peaks shift to lower temperatures as the proportion of the blend partner increases. The simultaneous crystallization of rPET and PBT hinders each other and leads to less organized crystals [33, 49, 53, 54]. A lower crystallization temperature offers an advantage in welding processes, as less energy is required [30].

Additionally, as depicted in Fig. 4b, the crystallization temperature decreases as the blend ratio approaches rPET-50PBT50. The lowest crystallization temperature of 142 °C is observed in rPET60PBT40. This lower temperature requirement for crystallization is essential due to the phase separation needed for both polymers from the miscible melt phase [55, 56]. This reduction in crystallization temperature widens the foaming window, providing more flexibility in the welding process. When combined with the relatively rapid crystallization rate of PBT [28], the rPET40PBT60 formulation exhibits the best expansion rate and uniform cell structures, attributed to stabilization via crystallization [11, 57, 58].

Conclusion

Bead foams derived from rPET/PBT with a pronounced double melting peak were processed by extrusion foaming. The effect of both CE modification and blend ratio on morphology and foam density were systematically investigated. The results showed that increasing the CE concentration up to 0.8 wt.-% in the rPET50PBT50 blend led to remarkable improvements in morphology and density compared to the unmodified blend. Specifically, an average cell size

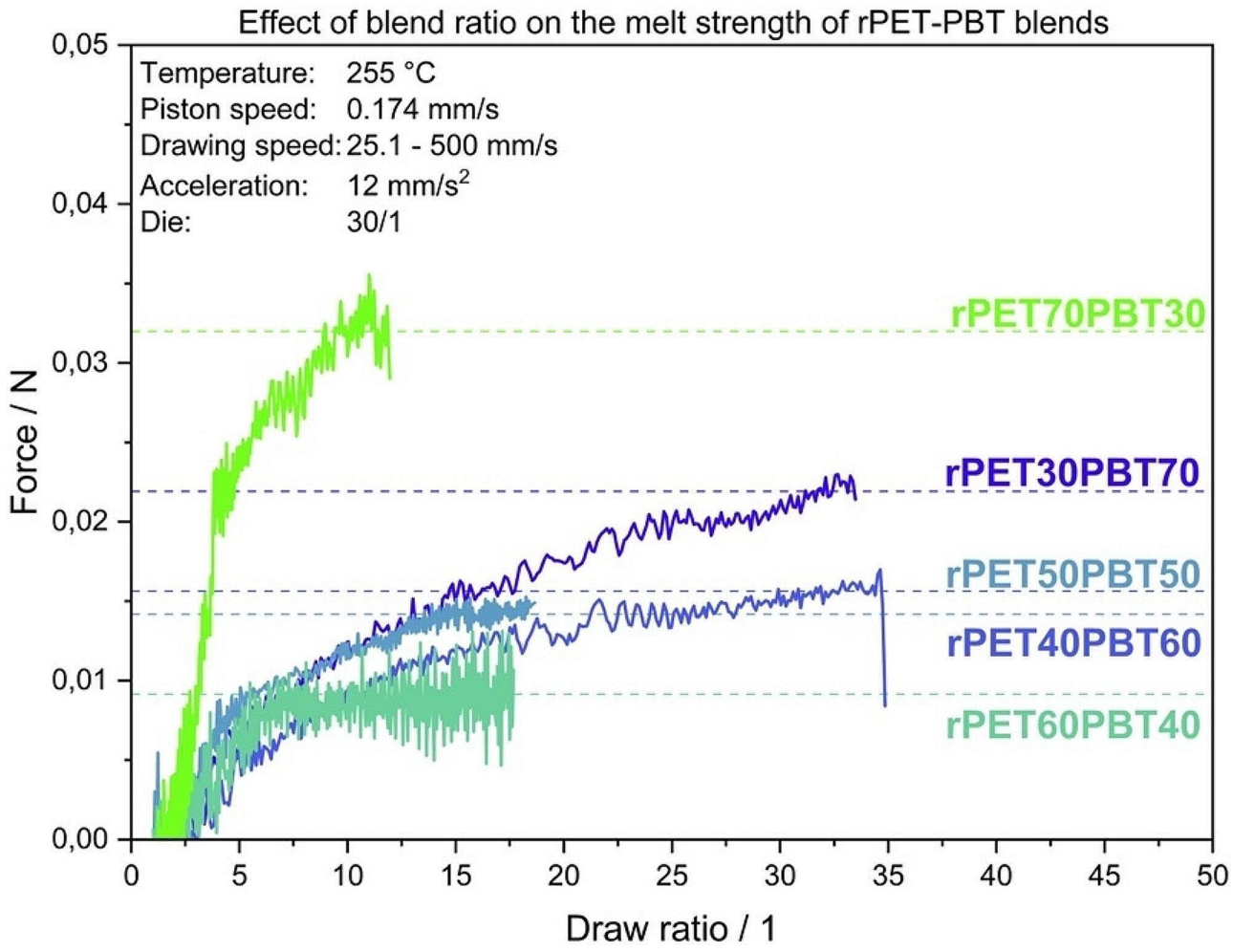

Fig. 3 Effect of blend ratio on the melt strength of rPET-PBT blends

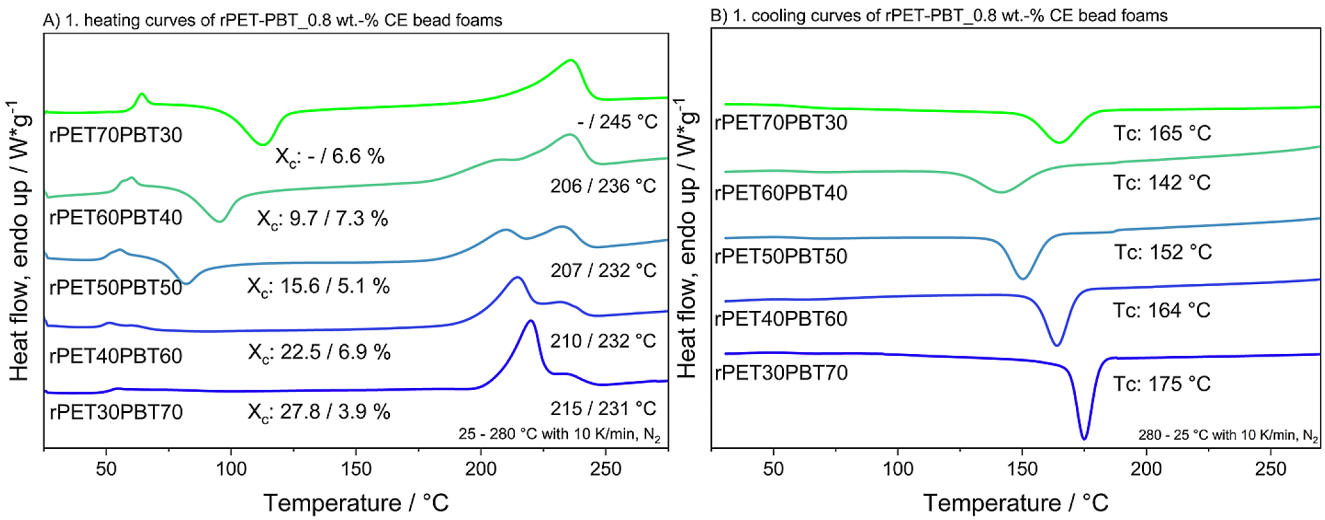

Fig. 4 1. Heating (**A**) and cooling (**B**) curves of rPET-PBT foams with varied blend ratio

of 107 ± 17 µm and a density of 182 kg/m^3 were achieved, which corresponds to an overall weigth reduction of 86.4% compared to the bulk material. Further improvements were achieved by adjusting the blend ratio, which influenced both the density and the morphology. A higher PBT content led to lower density and therefore a higher expansion rate. Conversely, varying the rPET content up to 70 wt.-% showed no significant effect. The optimum balance between density and cell size was found for rPET40PBT60, which had a foam density of 170 kg/m^3 and an average cell size of 108 ± 23 µm. The addition of CE up to 0.8wt.-% has a positive effct onf foam formation as both melt strength and elongation were improved. DSC analysis showed double melting peak formation in blends except in rPET70PBT30 while crystallization temperature was lowest in rPET50PBT50.

Supplementary Information The online version contains supplementary material available at https://doi.org/10.1007/s10924-024-03360-z.

Acknowledgements The authors would like to acknowledge the Bavarian Polymer Institute (BPI) for providing access to different analysis methods. Special thanks to Ute Kuhn, Annika Pfaffenberger and Sebastian Gröschel for their support during the trials.

Author Contributions A.H.: Conceptualization, methodology, data curation and analysis, writing original manuscript, Y.A.: Support writing original manuscript, M.R.: Review the original articles and funding acquisition, H.R.: Conceptualization, review the original articles, supervision, project administration and funding acquisition.

Funding Open Access funding enabled and organized by Projekt DEAL.
The authors would like to thank German Research Foundation (DFG) with the grant number AL 474/51-1 and the Scientific and Technological Research Council of Turkey (TUBITAK) in the context of 2507 project with the project number of 220N342 for funding the project.

Data Availability No datasets were generated or analysed during the current study.

Declarations

Conflict of interest The authors declare no competing interests.

References

1. Guo Y, Hossieny N, Chu RKM, Park CB, Zhou N (2013) Critical processing parameters for foamed bead manufacturing in a lab-scale autoclave system, Elsevier. (n.d.). (accessed December 18, 2023). https://www.sciencedirect.com/science/article/pii/S1385894712013800
2. Nofar M, Guo Y, Park CB (2013) Double crystal melting peak generation for expanded polypropylene bead foam manufacturing. Ind Eng Chem Res 52:2297–2303. https://doi.org/10.1021/IE302625E
3. Himmelsbach A, Standau T, Meuchelböck J, Altstädt V, Ruckdäschel H (2022) Approach to quantify the resistance of polymeric foams against thermal load under compression. J Polym Eng. https://doi.org/10.1515/POLYENG-2021-0312
4. Guo B, Chan C (1998) Chain extension of poly (butylene terephthalate) by reactive extrusion, J. Appl. Polym. Sci. 71:1827–1834
5. Karsli NG (2017) A study on the fracture, mechanical and thermal properties of chain extended recycled poly(ethylene terephthalate). J Thermoplast Compos Mater 30:1157–1172. https://doi.org/10.1177/0892705715618740
6. Standau T, Schreiers P, Hilgert K, Altstädt V (2020) Properties of bead foams with increased heat stability made from the engineering polymer polybutylene terephthalate (E-PBT). AIP Conf Proc 2205:1–6. https://doi.org/10.1063/1.5142954
7. Köppl T, Raps D, Altstädt V (2014) Bead foaming of poly(butylene terephthalate) by underwater pelletizing. J Cell Plast 50:475–487. https://doi.org/10.1177/0021955X14528524
8. Standau T, Hädelt B, Schreier P, Altstädt V (2018) Development of a bead foam from an Engineering Polymer with Addition of Chain Extender: expanded polybutylene terephthalate. Ind Eng Chem Res 57:17170–17176. https://doi.org/10.1021/acs.iecr.8b04799
9. Kuhnigk J, Krebs N, Mielke C, Standau T, Pospiech D, Ruckdäschel H (2022) Influence of Molecular Weight on the bead foaming and Bead Fusion Behavior of Poly(butylene terephthalate) (PBT). Ind Eng Chem Res. https://doi.org/10.1021/acs.iecr.2c03233
10. Kuhnigk J, Standau T, Dörr D, Brütting C, Altstädt V, Ruckdäschel H (2022) Progress in the development of bead foams– A review. J Cell Plast 58:707–735. https://doi.org/10.1177/0021955X221087603
11. Nofar M, Park CB (2014) Poly (lactic acid) foaming. Prog Polym Sci 39:1721–1741. https://doi.org/10.1016/J.PROGPOLYMSCI.2014.04.001
12. Bethke C, Goedderz D, Weber L, Standau T, Döring M, Altstädt V (2020) Improving the flame-retardant property of bottle-grade PET foam made by reactive foam extrusion. J Appl Polym Sci 137:49042. https://doi.org/10.1002/app.49042
13. Aksit M, Zhao C, Klose B, Kreger K, Schmidt HW, Altstädt V (2019) Extruded Polystyrene Foams with Enhanced Insulation and Mechanical Properties by a Benzene-Trisamide-Based Additive. Polym. https://doi.org/10.3390/POLYM11020268
14. Standau T, Nofar M, Dörr D, Ruckdäschel H, Altstädt V (2021) A review on multifunctional epoxy-based Joncryl® ADR Chain Extended Thermoplastics. Polym Rev 62:1–55. https://doi.org/10.1080/15583724.2021.1918710
15. Yang Z, Xin C, Mughal W, Wang Z, Bai X, He Y (2018) Prediction of foamability of polyethylene terephthalate using viscous and elastic parameters. Adv Polym Technol 37:2344–2353. https://doi.org/10.1002/ADV.21910
16. Standau T, Zhao C, Castellón SM, Bonten C, Altstädt V (2019) Chemical modification and foam processing of polylactide (PLA). Polym (Basel). https://doi.org/10.3390/polym11020306

17. Wang Z, Xu D, Bai S, Li S (2023) Foaming behaviors and mechanical properties investigation of high-strength polyethylene terephthalate/polycarbonate bead foam. J Appl Polym Sci 140:e54558. https://doi.org/10.1002/APP.54558
18. Colby RH, Fetters LJ, Graessley WW (1987) Melt viscosity-Molecular Weight Relationship for Linear polymers. Macromolecules 20:2226–2237. https://doi.org/10.1021/MA00175A030
19. Härth M, Kaschta J, Schubert DW (2014) Shear and Elongational Flow properties of Long-Chain branched poly(ethylene terephthalates) and correlations to their molecular structure. Macromolecules 47:4471–4478. https://doi.org/10.1021/ma5002657
20. Costa ARM, Almeida TG, Silva SML, Carvalho LH, Canedo EL (2015) Chain extension in poly(butylene-adipate-terephthalate). Inline testing in a laboratory internal mixer. Polym Test 42:115–121. https://doi.org/10.1016/j.polymertesting.2015.01.007
21. Standau T, Nofar M, Dörr D, Ruckdäschel H, Altstädt V (2022) A review on multifunctional epoxy-based Joncryl® ADR Chain Extended Thermoplastics. Polym Rev 62:296–350. https://doi.org/10.1080/15583724.2021.1918710
22. Himmelsbach A, Standau T, Kuhnigk J, Bubmann T, Akdevelioglu Y, Nofar M, Ruckdäschel H (2023) Investigation of the Reaction Kinetics of poly(butylene terephthalate) and Epoxide Chain Extender. Macromol Mater Eng 308:2200683. https://doi.org/10.1002/MAME.202200683
23. Guclu M, Alkan Göksu Y, Özdemir B, Ghanbari A, Nofar M (2022) Thermal stabilization of recycled PET through Chain Extension and blending with PBT. J Polym Environ 30:719–727. https://doi.org/10.1007/s10924-021-02238-8
24. Nofar M, Oğuz H (2019) Development of PBT/Recycled-PET blends and the influence of using Chain Extender. J Polym Environ 27:1404–1417. https://doi.org/10.1007/s10924-019-01435-w
25. Brütting C, Dreier J, Bonten C, Altstädt V, Ruckdäschel H, Behavior (2023) Sustainable Immiscible Polylactic Acid (PLA) and Poly(3-hydroxybutyrate-co-3-hydroxyvalerate) (PHBV) Blends: Crystallization and Foaming Behavior. ACS Sustain Chem Eng 11:6676–6687. https://doi.org/10.1021/ACSSUSCHEMENG.3C00199
26. Mielke C, Pospiech D, Kuhnigk J, Korwitz A, Komber H, Bernhardt R, Krebs N, Boldt R, Ruckdäschel H, Voit B, Mielke C, Pospiech D, Korwitz A, Komber H, Bernhardt R, Boldt R, Voit B, Kuhnigk J, Krebs N, Ruckdäschel H (2023) Partially Bio-based Polyester Bead foams via Extrusion Foaming of Poly(butylene terephthalate)/Poly(butylene furanoate) blends. Macromol Mater Eng 308:2300281. https://doi.org/10.1002/MAME.202300281
27. Zhang R, Xiong Y, Liu Q, Hu S (2017) Improved cell morphology and thermal properties of expanded polypropylene beads by the addition of PP with a high melting point. J Appl Polym Sci 134:45121. https://doi.org/10.1002/APP.45121
28. Kuhnigk J, Raps D, Standau T, Luik M, Altstädt V, Ruckdäschel H (2021) Insights into the Bead Fusion mechanism of expanded polybutylene terephthalate (E-PBT). Polym (Basel) 13:582. https://doi.org/10.3390/polym13040582
29. Raps D, Hossieny N, Park CB, Altstädt V (2015) Past and present developments in polymer bead foams and bead foaming technology. Polym (Guildf) 56:5–19. https://doi.org/10.1016/J.POLYMER.2014.10.078
30. Dippold M, Töpfer C, Ruckdäschel H (2023) Influence of dielectric properties of polybutylene terephthalate and respective foam beads on process behavior in radio-frequency welding. J Appl Polym Sci. https://doi.org/10.1002/APP.54988
31. Nofar M, Ameli A, Park CB (2015) Development of polylactide bead foams with double crystal melting peaks. Polym (Guildf) 69:83–94. https://doi.org/10.1016/j.polymer.2015.05.048
32. Akdevelioğ Lu Y, Himmelsbach A, Ruckdäschel H, Nofar M (2024) Melt Rheological and Bead foaming behavior of recycled polyethylene Terephthalate/Polybutylene terephthalate blends modified with a Joncryl Chain Extender. Ind Eng Chem Res. https://doi.org/10.1021/ACS.IECR.3C03371
33. Himmelsbach A, Brütting C, Akdevelioglu Y, Albuquerque RQ, Nofar M, Ruckdäschel H (2024) Non-isothermal crystallization kinetic of recycled<scp>PET and its blends with <scp>PBT modified with epoxy-based multifunctional chain extender. J Appl Polym Sci. https://doi.org/10.1002/app.55357
34. Awaja F, Pavel D (2005) Recycling of PET. Eur Polym J 41:1453–1477. https://doi.org/10.1016/j.eurpolymj.2005.02.005
35. Al-Itry R, Lamnawar K, Maazouz A (2014) Rheological, morphological, and interfacial properties of compatibilized PLA/PBAT blends. Rheol Acta 53:501–517. https://doi.org/10.1007/s00397-014-0774-2
36. Dhavalikar R, Xanthos M (2003) Parameters affecting the chain extension and branching of PET in the melt state by polyepoxides. J Appl Polym Sci 87:643–652. https://doi.org/10.1002/app.11425
37. Jacques B, Devaux J, Legras R, Nield E (1997) Reactions induced by triphenyl phosphite addition during melt mixing of PET/PBT blends: chromatographic evidence of a molecular weight increase due to the creation of bonds of two different natures. Polym (Guildf) 38:5367–5377. https://doi.org/10.1016/S0032-3861(97)00097-9
38. Ge Y, Yao S, Xu M, Gao L, Fang Z, Zhao L, Liu T (2019) Improvement of poly(ethylene terephthalate) melt-foamability by long-chain branching with the combination of Pyromellitic Dianhydride and Triglycidyl Isocyanurate. Ind Eng Chem Res 58:3666–3678. https://doi.org/10.1021/acs.iecr.8b04157
39. Parky CP, Garcia GA (2002) Development of polypropylene plank foam products. J Cell Plast 38:219–228. https://doi.org/10.1177/0021955X02038003268
40. Härth M, Dörnhöfer A, Kaschta J, Münstedt H, Schubert DW (2021) Molecular structure and rheological properties of a poly(ethylene terephthalate) modified by two different chain extenders. J Appl Polym Sci 138:50110. https://doi.org/10.1002/app.50110
41. Odet F, Ylla N, Delage K, Cassagnau P (2022) Influence of Chain extenders on Recycled Standard and Opaque PET Rheology and Melt-Spun Filament properties. ACS Appl Polym Mater 4:8290–8302. https://doi.org/10.1021/ACSAPM.2C01231
42. Incarnato L, Scarfato P, Di Maio L, Acierno D (2000) Structure and rheology of recycled PET modified by reactive extrusion. Polym (Guildf) 41:6825–6831. https://doi.org/10.1016/S0032-3861(00)00032-X
43. Kim E, Kweon MS, Romero-Diez S, Gupta A, Yan X, Spofford C, Pehlert G, Lee PC (2021) Effects of pressure drop rate and CO2 content on the foaming behavior of newly developed high-melt-strength polypropylene in continuous extrusion. J Cell Plast 57:413–432. https://doi.org/10.1177/0021955X20943110
44. Weingart N, Raps D, Kuhnigk J, Klein A, Altstädt V (2020) Expanded Polycarbonate (EPC)—A New Generation of High-Temperature Engineering Bead Foams. Polym. https://doi.org/10.3390/POLYM12102314
45. Aravinthan G, Kale DD (2005) Blends of poly(ethylene terephthalate) and poly(butylene terephthalate). J Appl Polym Sci 98:75–82. https://doi.org/10.1002/app.22017
46. Stocco A, Carrubba VL, Piccarolo S, Brucato V (2009) The solidification behavior of a PBT/PET blend over a wide range of cooling rate. J Polym Sci Part B Polym Phys 47:799–810. https://doi.org/10.1002/polb.21687
47. Stein R.S, Khambatta F.B, Warner F.P, Russell T, Escala A, Balizer E (1978) X-ray and optical studies of the morphology of polymer blends. J Polym Sci Polym Symp 63:313–328. https://doi.org/10.1002/POLC.5070630126
48. Liang H, Xie F, Guo F, Chen B, Luo F, Jin Z (2008) Non-isothermal crystallization behavior of poly(ethylene terephthalate)/

Poly(trimethylene terephthalate) blends. Polym Bull 60:115–127. https://doi.org/10.1007/s00289-007-0832-3
49. Mishra SP, Deopura BL (1985) Crystallization behaviour of poly(ethylene terephthalate) and poly(tetramethylene terephthalate) blends. Die Makromol Chemie 186:641–647. https://doi.org/10.1002/MACP.1985.021860317
50. Li Y, Yao Z, Chen ZH, Cao K, Qiu SL, Zhu FJ, Zeng C, Huang ZM (2011) Numerical simulation of polypropylene foaming process assisted by carbon dioxide: Bubble growth dynamics and stability, Elsevier. (n.d.). https://www.sciencedirect.com/science/article/pii/S0009250911002892 (accessed December 20, 2023)
51. Badia JD, Strömberg E, Karlsson S, Ribes-Greus A (2012) The role of crystalline, mobile amorphous and rigid amorphous fractions in the performance of recycled poly (ethylene terephthalate) (PET), Polym. Degrad Stab 97:98–107. https://doi.org/10.1016/J.POLYMDEGRADSTAB.2011.10.008
52. Dangseeyun N, Supaphol P, Nithitanakul M (2004) Thermal, crystallization, and rheological characteristics of poly(trimethylene terephthalate)/poly(butylene terephthalate) blends. Polym Test 23:187–194. https://doi.org/10.1016/S0142-9418(03)00079-5
53. Zeng J-B, Zhu Q-Y, Li Y-D, Qiu Z-C, Wang Y-Z (2010) Unique Crystalline/Crystalline Polymer Blends of Poly(ethylene succinate) and poly(p -dioxanone): miscibility and crystallization behaviors. J Phys Chem B 114:14827–14833. https://doi.org/10.1021/jp104709z
54. Yoshie N, Asaka A, Inoue Y (2004) Cocrystallization and phase segregation in Crystalline/Crystalline polymer blends of bacterial copolyesters. Macromolecules. https://doi.org/10.1021/ma049858p
55. Escala A, Stein RS (1979) Crystallization Studies of Blends of Polyethylene Terephthalate and Polybutylene Terephthalate. ACS Publications. https://doi.org/10.1021/ba-1979-0176.ch024
56. Eitouni HB, Balsara NP, Blends TofP (2007) Phys Prop Polym Handb. https://doi.org/10.1007/978-0-387-69002-5_19
57. Liu B, Jiang T, Zeng X, Deng R, Gu J, Gong W, He L (2021) Polypropylene/thermoplastic polyester elastomer blend: crystallization properties, rheological behavior, and foaming performance. Polym Adv Technol 32:2102–2117. https://doi.org/10.1002/PAT.5240
58. Reignier J, Gendron R, Champagne MF (2007) Autoclave foaming of poly(ε-Caprolactone) using carbon dioxide: impact of crystallization on cell structure. J Cell Plast 43:459–489. https://doi.org/10.1177/0021955X07079591

Authors and Affiliations

Andreas Himmelsbach[1] · Yavuz Akdevelioglu[2] · Mohammadreza Nofar[2] · Holger Ruckdäschel[1]

✉ Holger Ruckdäschel
ruckdaeschel@uni-bayreuth.de; holger.ruckdaeschel@uni-bayreuth.de

[1] Department of Polymer Engineering, University of Bayreuth, Bayreuth, Germany

[2] Sustainable & Green Plastics Laboratory, Metallurgical & Materials Engineering Department, Faculty of Chemical and Metallurgical Engineering, Istanbul Technical University, Istanbul 34469, Turkey